Electronic Supporting Information

Albumin Removal from Human Serum using Surface Nanopockets on Silica-coated Magnetic Nanoparticles

Snehasis Bhakta,[†] Chandra K. Dixit,[†] Itti Bist,[†] John Macharia,[†] Min Shen,[†] Karteek Kadimisetty,[†] Junkai He,[†] Biswanath Dutta,[†] Steven L. Suib[*,†,§] James F. Rusling[*,†,§,⊥,‖]

[†]Department of Chemistry, University of Connecticut, Storrs, Connecticut 06269-3060

[§]Institute of Materials Science, University of Connecticut, Storrs, Connecticut 06269-3136

[⊥]Department of Cell Biology, University of Connecticut Health Center, Farmington, Connecticut 06030

[‖]School of Chemistry, National University of Ireland at Galway, Galway, Ireland

*Corresponding Authors:

Email: james.rusling@uconn.edu Phone number: (860) 486-4909; Fax: (860) 486-2981

Steven.suib@uconn.edu Phone number: (860) 486-2797; Fax: (860) 486-2981

Chemicals and Materials. Tetraethylorthosilicate (TEOS, ≥99%), (3-aminopropyl)-triethoxysilane (APTES, ≥98%), glutaraldehyde (Grade I, 25% in water), human serum albumin (HSA, lyophilized powder), lysozyme (lyophilized powder), bovine serum albumin (BSA, lyophilized powder), hydrochloric acid (ACS reagent 37%), sodium hydroxide, triton X-100, TWEEN 20, sodium phosphate dibasic and sodium phosphate monobasic, BCA assay (Bicinconinic acid), propyl-N-ethylcarbodiimide (EDC), N-Hydroxysulfosuccinimide (NHSS), human serum, Fluorescein isothiocyanateand (FITC) and glycine were from Sigma–Aldrich. Hydroxymethyltriethoxysilane (HMTEOS), n-propyltriethoxysilane (PTES), benzyltriethoxysilane (BTES) were from Gelest, Inc. Silica modified SiO_2@Fe_2O_3 paramagnetic nanoparticles was from Chemicell. Human antibody (anti-VEGF) and anti-human serum albumin (anti-HSA) were purchased from R&D systems. The surface plasmon resonance (SPR) chip functionalized with polyethylene glycol/carboxyl was from Reichert Technologies Life Sciences (part number 13206061). HPLC-grade water, acetonitrile and formic acid were obtained from Sigma. Methyl-PEG-NHS ester (MeO-PEG_4-NHS) was bought from Thermo Fisher Scientific. All solutions were prepared using 18 MΩ cm water purified by passing house-distilled water through a Hydro Service and Supplies purification system. Solutions were passed through 0.45 μm filters (Fisher) before use. Buffer for most experiments was 10 mM phosphate, pH 7.3.

Instrumentation. Scanning Electron Microscopy (SEM) was performed with a Teneo LVSEM from FEI. Dynamic Light Scattering (DLS) was done with an ALV/CGS-3. Zeta potential measurements were done using ZetaPlus (Brookhaven Instruments Corp.) Zeta potential analyzer. Absorption spectra were obtained on a HP8453 UV–visible spectrophotometer (Agilent Technologies, Santa Clara, CA). The surface plasmon resonance (SPR) experiments were done with a Reichert Analytical Instruments SPR700DC dual channel flow spectrometer on a gold SPR chips prefunctionalized with a mixed monolayer (10% COOH-$(PEG)_6$-alkanethiol and 90% OH-$(PEG)_3$-alkanethiol) at 25ºC.

Micro-Synthesis of HSA-binding NPs. A 2 mg magnetic particles dispersion was reacted in a 1 mL Eppendorf tube. The amount of proteins required to cover the surface was optimized based on the number of particles. Briefly, 2 mg magnetic particles contained $4x10^{11}$ particle and 1

particle have a maximum 450 human serum albumin (HSA) onto the surface of magnetic particle. Concentrations for template protein HSA was taken as 10 μg/mL, 5 μg/mL, 1 μg/mL, 0.5 μg/m and 20 μg/mL for the synthesis of HSA-binding nanoparticle (NPs). At first, 2 mg of magnetic particles was dispersed in 1 mL phosphate buffer, pH 7.8. The particle was washed 3 times using a magnet and followed by reconstituting the separated particle in the same buffer. The phosphate buffer at pH 7.8 was chosen as homobifunctional glutaraldehyde works better in the pH range of 7.5 to 8.0. Then, HSA solution (different template concentration from 0.5 μg/mL to 20 μg/mL as mentioned above) was added into the nanoparticle suspension and mixed for 10 mins in a rotor. Then, 100 μL of 22.7 mM glutaraldehyde solution was added for cross-conjugation. The final volume for the reaction was 1 mL with final glutaraldehyde concentration of 2.27 mM. After 1 h, 10 μL of 1 M Tris-HCl at pH 8.0 was added to terminate the reaction. The mixture was then washed with pH 7.3 phosphate buffer 3 times with particles isolated using a magnet and then reconstituted to 1 mL in the same buffer for further reaction. 100 μL of 0.4 M tetraethyl orthosilicate solution was then added to react with these particles for 1 h using a rotor, followed by addition of 5 μL of n-propyltriethoxysilane (0.4 M), 5 μL of benzyltriethoxysilane (0.4 M), 5 μL of hydroxymethyltriethoxysilane (0.4 M) and 10 μL of (3-aminopropyl)-triethoxysilane (0.4 M) monomer solution. The subsequent reaction was done in a rotor for another 6 h to construct the polymer layers with nanopockets around the proteins. The probable mechanism of the polymerization that leads to HSA-specific nanopockets on the surface of silica-coated magnetic nanoparticles is described in Figure S1.

After 6 h, the particles were washed 3 times with phosphate buffer pH 7.3 followed by reconstituting in 50 mM NaOH solution with 0.01% Triton X-100 to remove bound HSA from the particles. The solution was ultrasonicated for 5 min followed by incubation for another 15 min. Finally, the solution was sonicated for 1 min and the particles were washed thoroughly with phosphate buffer pH 7.3 for 5 times to remove all proteins. Finally, the HSA-binding NPs were reconstituted in phosphate buffer and stored at 4 ºC for further use.

Protein binding BCA Assay. The amount of protein bound was measured using a bicinchoninic acid (BCA) total protein assay.[1] In brief, suspension of HSA-binding NPs was mixed in an HSA

solution in a rotor for an hour. Then paramagnetic NPs were separated using a magnet followed by washing with phosphate buffer for 3 times. BCA solution was then added in the conjugates and incubated for 15 mins at 60ºC. The absorbance was measured at 562 nm for protein bound on the NPs and from that amount of protein bound on the particle was calculated.

Binding constants were estimated using the Langmuir-Freundlich equation for protein binding to multiple sites on particles.[2,3]

$$X/X_m = \mathbf{K_{LF}}C^{1/n}/(1+ \mathbf{K_{LF}}C^{1/n}) \quad (1)$$

Where X is concentration of protein bound/mg of NP, X_m is maximum concentration of protein bound, $\mathbf{K_{LF}}$ is the binding constant, C is concentration of protein in solution, and n is an empirical constant between 0.4 and 0.5 for protein adsorption onto solid surfaces. It is important to realize the $\mathbf{K_{LF}}$ is not the same as the classical binding constant $\mathbf{K_B}$ (M^{-1}) for binding of one protein to an antibody. However, but $\mathbf{K_{LF}}$ provides a practical measurement directly related to $\mathbf{K_B}$ that can be used to compare binding efficiencies. Expressing experimental data as X'= X/Xm and C' = $C^{1/n}$, $\mathbf{K_{LF}}$ was estimated by non-linear regression of isotherm data onto eq 1. Larger values of $\mathbf{K_{LF}}$ represent larger binding affinities. The binding capacity of the synthesized NPs was determined by allowing to bind a known concentration of HSA and retrieving the bound concentration as measured with BCA assay. The values were presented as mg proteins bound per g NPs.

For binding of HSA to monoclonal anti-HSA, the K_D is reported as 4.7 nM.[4] The K_{LF} value for HSA-binding NP was estimated by fitting to eq 1 above as 1.75 x 10^5 $(mL/mg)^{1/n}$ where n is 0.46. We converted the K_{LF} to K_D to get an idea about the binding strength of the HSA-binding NPs relative to native monoclonal antibodies. There are multiple surface nanopockets on the nanoparticle and the experimental average value is 250, based on binding capacity measured by using a fluorescence tagged HSA. Next, we have calculated probable number of binding pockets in 2 mg silica coated magnetic nanoparticles. The value is calculated as 1.0 x 10^{14} pockets which is approximately 0.2 nanomoles. (number of moles is total number binding pockets dividing by Avogadro's number). The total volume is 1 mL i.e. 10^{-3} L. The molarity of suspension is ~200 nM as molarity =moles/Liter of solution, or 100 nM for 1 mg/mL dispersions.

Then, we take the K_{LF} and convert it for the corresponding molarity of nanopockets in the dispersion.

$K_{LF}=1.80 \times 10^5$ $(mL/mg)^{2.22}$; 1/n=2.22

$K_{LF}= 1.80 \times 10^5$ $(1/100)^{2.22}$ $nM^{-2.22}$ since 1 mg/mL is equivalent to 100 nM

$K_{LF}=6.53$ $nM^{-2.22}$

$K_D \approx 1/K_{LF}= 0.15$ $nM^{2.22}$ or

$K_D \approx 2.22$ root of $1/K_{(LF)}$, which is equivalent to K_D of an antibody (units in nM).

$K_D \approx 0.43$ nM

Gel Electrophoresis. Sodium dodecyl sulfate (SDS) PAGE was run to study the depleted samples. SDS-PAGE was performed in a Bio-Rad Mini-Protean electrophoresis apparatus using a standard protocol.[5] In all experiments, 10% polyacrylamide gel was used as separating gel with a 5% stacking gel. The samples were mixed with loading buffer (Tris buffer pH 6.8 containing 2% w/v SDS, 10% v/v β-mercaptoethanol) in 3:1 ratio and kept in boiling water for 5 minutes. Samples were loaded such that each well contained about 5 µg of proteins. Then the gel was run for 1 h at 200 V for effective separation of proteins. Different bands were visualized by treating with staining solution (50% methanol, 10% acetic acid and 1% brilliant blue R250) for 30 minutes. Excess amount of dye was then destained by solution containing 50% methanol and 10% acetic acid. Finally, photographs were captured using a cell phone camera.

Binding experiment using FITC-tagged anti-HSA. To calculate the number of binding pockets and binding efficiency, fluorescence experiment was performed using FITC-tagged anti-HSA. In brief, FITC-tagged anti-HSA conjugate was first synthesized, mixed with HSA-bound NPs and finally fluorescence intensity was measured to measure amount of HSA bound on NPs. Anti-HSA was reacted with 10-fold molar excess of fluorescein isothiocyanate in 100 mM sodium bicarbonate buffer, pH 9.0. Briefly, 60 µL of 50 mM FITC was mixed with 50 µg/mL of anti-HSA and incubated for 5 h in dark under slow rotation in sodium bicarbonate buffer, pH 9.0. Volume was kept to 1 mL in all the reactions. Excess FITC was removed using a 3 kDa molecular cut off centrifugal filter tube (Millipore) and FITC-tagged anti-HSA conjugate was reconstituted in 10 mM phosphate buffer, pH 7.3. Then, HSA bound NPs conjugate was synthesized as described

above (the concentration of HSA was 10 µg/mL). Then, FITC-tagged anti-HSA (25 µg/mL) was mixed with the HSA-bound NPs conjugate and reacted for 2 h under continuous rotation. Finally, the NPs were separated, washed, reconstituted in phosphate buffer pH 7.3 and performed fluorescence measurement. Fluorescent intensity was measured using 495 nm excitation wavelength and 525 nm emission wavelength. Amount of HSA bound was measured from the fluorescence intensity. It was assumed that there was 1:1 binding between anti-HSA and HSA. Amount of albumin removed by ProteoExtract was measured in a similar way from the fluorescence intensity. (**Figure S7**).

Surface Plasmon Resonance studies (SPR). SPR was done at 25 °C using phosphate buffer with 0.05% TWEEN-20 (pH 7.3) as flow buffer with the Au SPR chip attached to an injection valve with a 100 µL injection loop. In brief, proteins, (1 mg/mL) were first immobilized on the carboxyl functionalized gold surface using an amine coupling agent.[6] Carboxyl groups were activated using a 1:2 mixtures of freshly prepared 4 mg EDC (3-(N, N-dimethylamino) propyl-N-ethylcarbodiimide) and 11 mg NHSS (N-Hydroxysulfosuccinimide) by flowing for 10 min at 10 µL/min. Then, the proteins in buffer were immobilized by introduction at 5 µL/min for 1200 sec. Unreacted sites were blocked using 1 M Glycine at pH 8.0 buffer. HSA-binding NP dispersions in phosphate buffer pH 7.3 were injected into the SPR sensor cell via the sample injection loop to monitor binding to surface proteins at a 35 µL/min flow rate, allowing 200 s for association and 200 s for dissociation. Data were initially analyzed by fitting equations 1 and 2 to estimate the association binding constant k_a and dissociation rate constant k_d. However, binding of HSA-binding NPs to proteins did not show dissociation even after 7 h of dissociation time, and the data gave very poor fits to eq 2. to obtain the "on" rate constant $\boldsymbol{k_a}$, the initial rate of change in SPR signal vs. time during association was plotted against [HSA-binding NP] and the $\boldsymbol{k_a}$ was estimated from the slope (eq 5).

$$R_t = Ck_aR_{max}[1 - \exp((Ck_a+k_d)t)]/(Ck_a+k_d) \quad (2)$$

$$R_t = R_{max}\exp(-k_dt) \quad (3)$$

$$K_D = k_d/k_a \quad (4)$$

$$\Delta R/\Delta t = k_a[Ab] \quad (5)$$

Surface charge and size distribution. HSA-binding NP development was closely monitored for changes taking place due to polymerization on the nanoparticle surface. Aminated silica-coated magnetic nanoparticles were highly stable in the suspension (zeta-potential: 58.3±7 mV). Polymerization of the monomers surrounding the template protein on the particle surface resulted in an overall zeta potential drop (-30.6±3 mV). A decreased potential of approximately -20 mV was due to HSA binding on the NPs consistent with previously reported values.[7,8] In an effort to understand the relation of size and polymerization on the developed NPs, we have performed scanning electron microscopy (SEM) and dynamic light scattering (DLS) analyses. Observation of the coating by HRTEM, STEM and SEM on the nanoparticle surface (**Figure 2 in main article and Figure S7**) confirmed that the method successfully grafted monomers. In addition, the difference obtained in hydrodynamic radii of bare and polymer-coated nanoparticles confirmed the generation of a coat with a thickness of 6-18 nm (**Figure S2b**). The polydispersity indices for nanoparticle and nanopockets were 0.161 and 0.268, respectively. We obtained 134 nm as the average radii further increased to 134±9 nm for protein-bound NPs (**Figure S1c**) suggesting the presence of protein on the NP surface. The swelling is roughly consistent with the 11x8.5 nm oblate ellipsoid shape of HSA.[9]

However, the slightly larger increase in radius may also be related to additional polymer coat swelling after the hydrated protein is bound. Clearly, the situation is complex, and cannot be viewed simply as a globular protein binding to the outside of a spherical nanoparticle.

HSA-binding NPs were synthesized with different template concentration e.g. 0.5, 1, 5.0, 10 and 20 μg/mL and binding experiments were performed using the BCA assay of bound HSA on NPs as mentioned above to establish the best possible synthetic conditions. The Langmuir-Freundlich isotherm model was used to fit the data (equation 1) and apparent K_{LF} values were calculated for each HSA-binding NPs (**Figure S3**). From the data, the HSA-binding NP synthesized using 1.0 μg/mL template protein gave the larges K_{LF} and binding capacity (T**able S1).**

Table S1. Apparent binding constants and capacity for HSA-binding NPs synthesized using different concentration of template proteins by measuring amount of protein bound on NPs using a BCA assay and plotting the values using the Langmuir-Freundlich binding model.

HSA concentration	0.5 µg/mL	1.0 µg/mL	5.0 µg/mL	10 µg/mL	20 µg/mL
K_{LF} $(mL/mg)^{1/n}$	1.68×10^5	1.75×10^5	1.50×10^5	1.52×10^5	1.60×10^5
capacity (mg HSA /g)	19	20	18	18	18.5

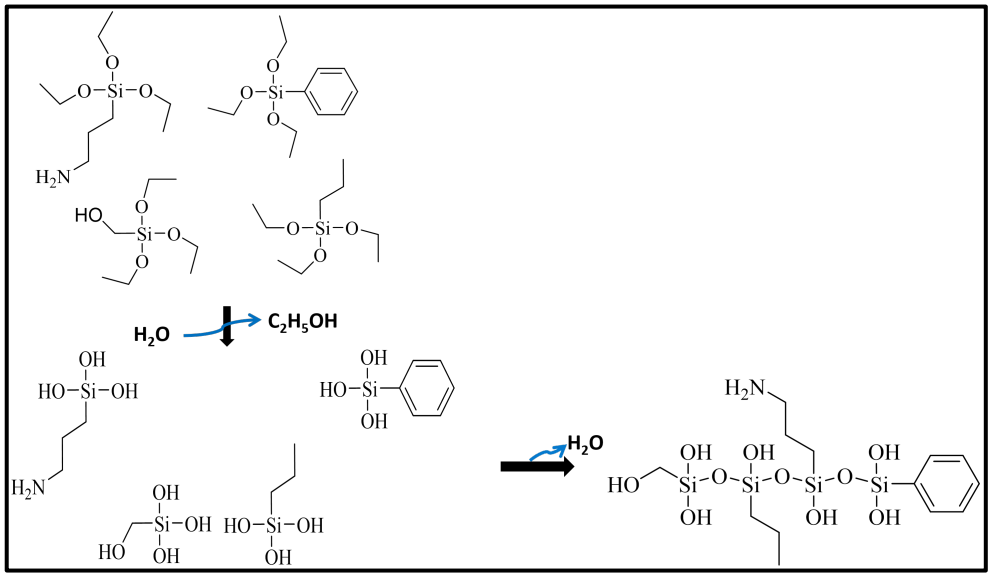

Figure S1: Schematic illustration of polymerization that leads to HSA-specific nanopockets on the surface of silica-coated magnetic nanoparticles.

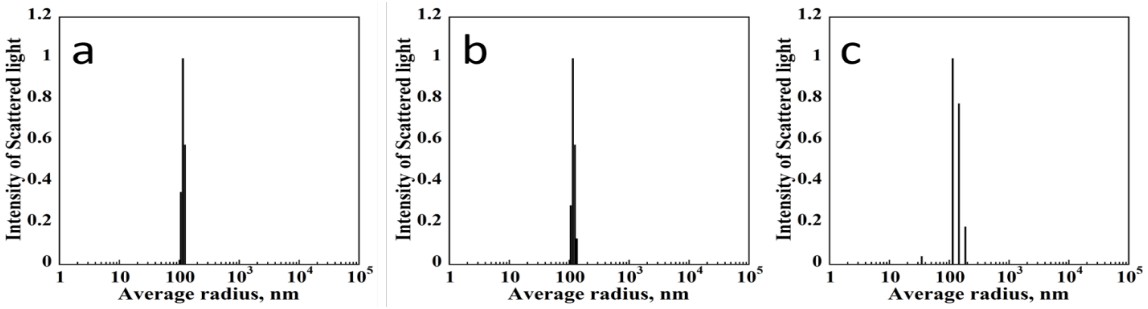

Figure S2: DLS hydrodynamic radii distributions. (a) SiO_2@Fe_2O_3 NPs, avg. radius 105 nm; (b) HSA-binding NPs, avg. radius 119 nm; (c) HSA-binding NPs with bound HSA, avg. radius 134 nm.

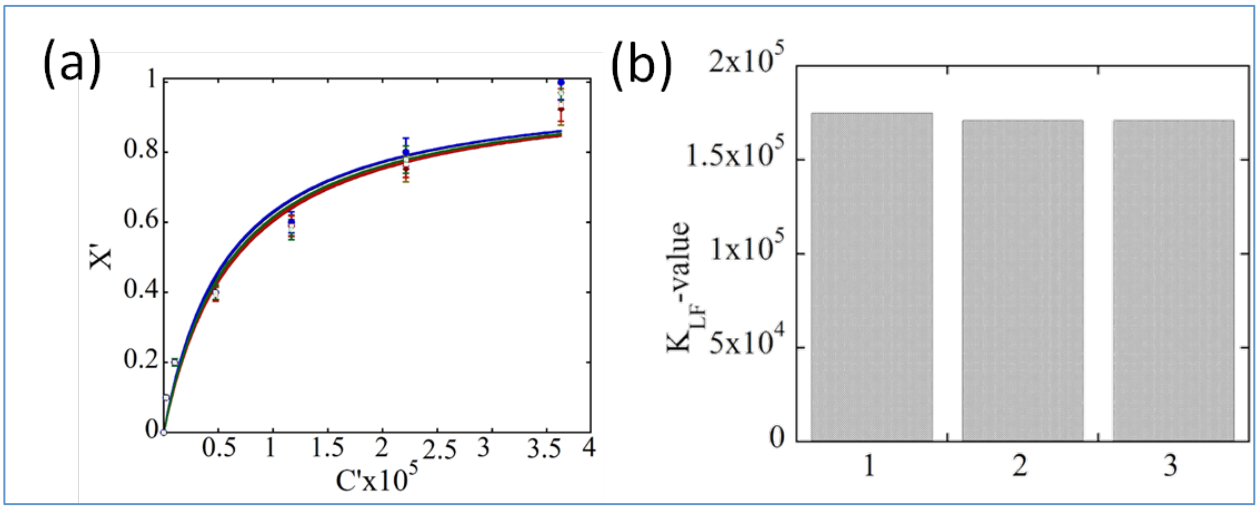

Figure S3. (a) Binding isotherms for HSA-binding NPs synthesized using different HSA concentrations. Amount of protein bound was measured using a BCA protein assay and data were fit to eq. 1 to obtain K_{LF} and capacity; (b) Representative apparent binding constants obtained for three different batches of HSA-specific nanopockets.

In a similar way, the selectivity of each HSA-binding NPs was measured to find out the best possible synthesized HSA-binding NPs for albumin separation from human serum sample. K_{LF} was measured for bovine serum albumin (BSA), non-homologous lysozyme and globulin anti-VEGF (IgG) to monitor the selectivity of each HSA-binding NP in the concentration range 0 to 10 μg/mL. The selectivity was best using 1 μg/mL HSA for NP synthesis compared to other HSA concentrations (**Table S2**). K_{LF} for this HSA-binding NP was 8 to 260 times better than the non-template proteins. Based on these studies, HSA-binding NP synthesized using 1 μg/mL HSA was selected for all further studies.

To improve selectivity, different concentration of MeO-PEG_4-NHS was added on the NPs before removing the template protein. The PEG derivative was treated for 30 minutes. Then, template protein was removed as described before and PEG-conjugated NPs was collected in phosphate buffer pH 7.3. The binding constant was measured for each proteins as described before. K_{LF} for this HSA-binding NP was 15 to 260 times better than the non-template proteins after adding

PEG monomer as described previously. Overall, the selectivity was best using 1 μg/mL HSA for NP synthesis and 0.5 mM MeO-PEG_4-NHS compared to other HSA concentrations (**Table S3**).

Table S2. The K_{LF}-values for HSA-binding NPs against different proteins

HSA (μg/mL)	K_{LF} $(mL/mg)^{1/n}$			
	HSA	BSA	Lysozyme	IgG
0.5	1.68×10^5	2.1×10^4	880	2.1×10^4
1.0	1.75×10^5	2.0×10^4	678	2.3×10^4
5.0	1.50×10^5	2.7×10^4	1.3×10^4	2.4×10^4
20	1.60×10^5	2.1×10^4	6698	2.3×10^4

Table S3. The K_{LF}-values for HSA-binding NPs treated with different concentration of MeO-PEG_4-NHS against different proteins (template HSA concentration was 1.0 μg/mL)

MeO-PEG_4-NHS mM	K_{LF} $(mL/mg)^{1/n}$			
	HSA	BSA	Lysozyme	IgG
0.1	1.75×10^5	2.0×10^4	734	2.3×10^4
0.5	1.80×10^5	1.04×10^4	701	1.2×10^4
2.0	1.61×10^5	2.2×10^4	6.95×10^3	3.2×10^4
5.0	1.54×10^5	4.96×10^4	7.92×10^4	8.3×10^4

The binding capacity of the commercial material, ProteoExtract HSA removal kit (Millipore) was also monitored. The material was first collected in an Eppendorf from the commercial column, then incubated with HSA as described before and finally amount of HSA bound was measured using both BCA assay and fluorescence experiment. The binding capacity was ~110 mg/g for ProteoExtract, whereas the binding capacity of the NPs was ~21 mg/g.

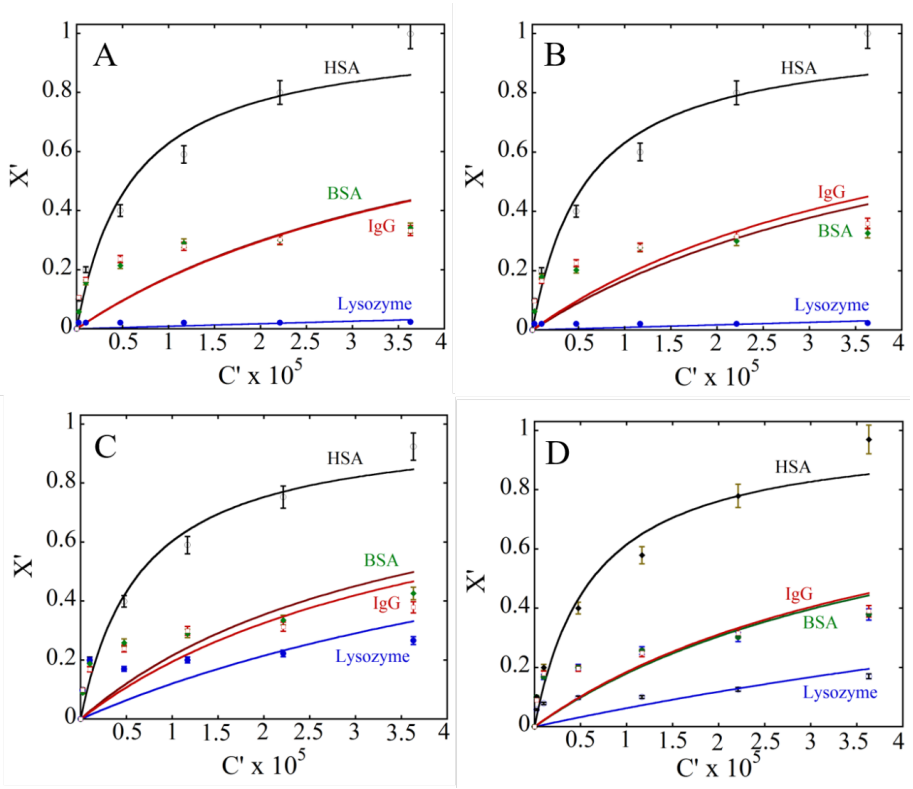

Figure S4. Binding studies of different against different proteins. Amount of proteins bound were measured using a BCA total protein assay and then Langmuir-Freundlich isotherm model was used to fit the data. (A) HSA-template protein 0.5 µg/mL, (B) HSA-template protein 1.0 µg/mL, (C) HSA-template protein 5.0 µg/mL, (D) HSA-template protein 20.0 µg/mL

Reproducibility of K_{LF}. Different batches of HSA-binding NP were synthesized using 1 µg/mL template protein concentration to check the reproducibility of the binding constant value. The protein-binding studies were performed under same condition and protein bound on the NP was measured using a BCA protein assay. K_{LF} values were very similar for all samples (**Figure S3b**).

Surface Plasmon Resonance (SPR). Binding of HSA-binding NP with HSA, BSA, lysozyme and IgG were also monitored by SPR. Proteins were immobilized on a PEG-self-assembled monolayer on Au SPR chips. The protein surface density on Au SPR chip was maintained at 7 x 10^9 proteins/mm^2. Then, dispersions of HSA-binding NP in pH 7.3 buffer were allowed to flow over the protein-bound chip in a flow cell. Data in Figure S4 shows rises in SPR signal due to binding

of HSA-binding NP to the immobilized proteins. After changing the flowing solution to buffer, the SPR signal became almost flat suggesting very little dissociation even after 7 h (data not shown). Maximum SPR binding signal was obtained for human serum albumin suggesting the specific binding towards template protein.

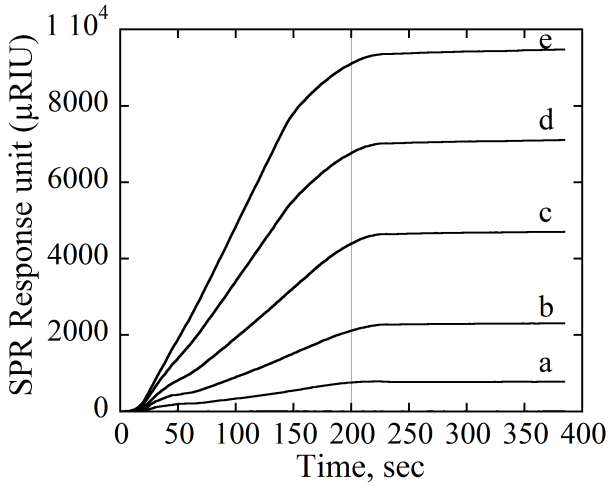

Figure S5. Examples of SPR responses at flow 35 μL/min for association (0-200 sec) and dissociation (200-400 sec) of HSA-binding NP suspension on an SPR chip with immobilized human serum albumin. HSA-binding NP dispersion was (a) 0.1 mg/mL; (b) 0.2 mg/mL; (c) 0.4 mg/mL; (d) 0.6 mg/mL and (e) 1 mg/mL.

Non-linear regression fits to the model in eqs 2 and 3 for the SPR data gave poor fits, most likely due to co-operative multivalent surface interactions. There is no dissociation even after 7 h of buffer flowing time which indicates strong binding. Thus, apparent association rate constants (k_a, eq 5) were estimated from initial slopes ($\Delta R/\Delta t$) of plots of $\Delta R/\Delta t$ vs. [HSA-binding NP] (**Figure 3b in main article**).[10] The apparent k_a was largest at 52.84 $(mg/mL)^{-1}sec^{-1}$ HSA binding, while lysozyme showed smaller k_a (5.22 $(mg/mL)^{-1}sec^{-1}$) and k_a for BSA and IgG were 6.30 and 8.10 $(mg/mL)^{-1}sec^{-1}$ respectively.

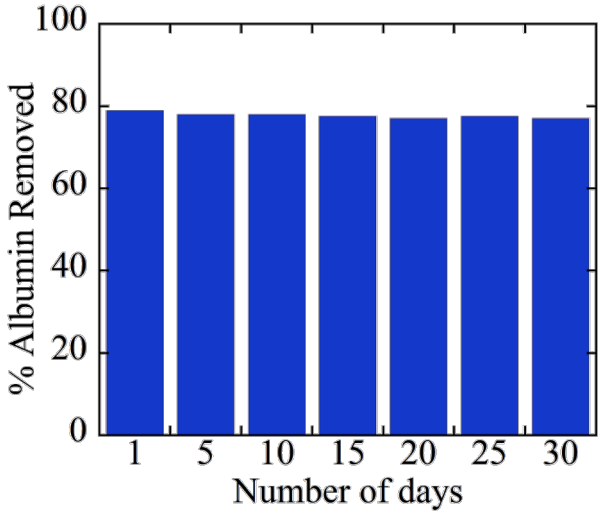

Figure S6. Illustrates the percentage of HSA removed from a serum sample using fresh batches of HSA-binding nanoparticles over a month after synthesis on day 0. NPs were stored in phosphate buffer pH 7.3 at 4°C.

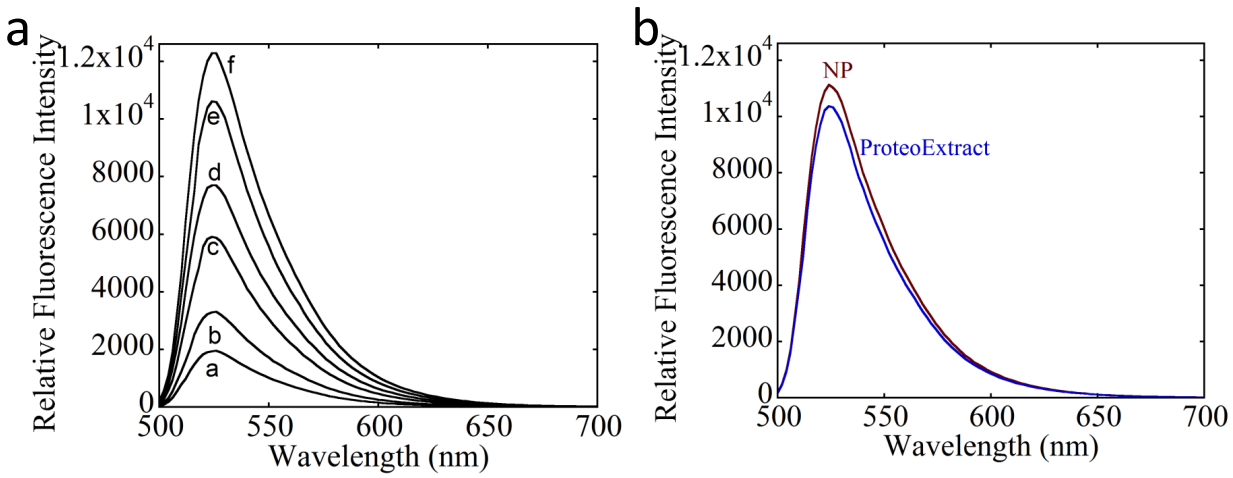

Figure S7. a. Fluorescence spectra for FITC-tagged anti-HSA at different concentration of anti-HSA in µg/mL. (a) 2.5, (b) 5, (c) 10, (d) 15, (e) 20 and (f) 25. b. The red line represents for HSA-bound NPs and FITC-tagged anti-HSA and blue line represents for HSA-bound ProteoExtract material FITC-tagged anti-HSA. Fluorescent intensity was measured using 495 nm excitation wavelength and 525 nm emission wavelength. Amount of albumin removed by NP was ~88% and by ProteoExtract material was ~84%.

Electron Microscopy for the nanopockets. Transmission electron microscopy/ scanning transmission electron microscopy (TEM/STEM) was used to find the surface morphology of the nanopockets in addition to SEM imaging. However, the effect of the magnetic field produced by the sample on the beam trajectory results in inevitable image distortions. Additionally, it is a practical restriction towards imaging magnetic nanoparticles because 4.8 mm is the closest Z-axis focus that we could achieve in SEM and at that focus it is hard to reveal any morphological aspects to that level. If we go closer, the powder particles (samples dried) can be sputtered by the beam and the particles could accumulate on the detector. For these reasons, we mimicked the binding sites on silica nanoparticles as described in the synthesis procedure to image morphological aspects at the binding pockets as well as possible. In addition, we attached HSA-conjugated gold nanoparticles (2-4 nm) onto the NPs as AuNP-HSA to bind specifically onto the nanopocket NP surfaces. The presence of small AuNPs may confirm the 'binding pockets' on the surface. **Figure 2A** in the main articles and **Figure S8(D)** show very smooth surfaces for the unreacted, bare silica nanoparticles whereas after the polymerization reaction, the surface morphology changes and the polymer coating can be observed for coated NPs (**Figure 2B and**

2C in main article). The rough surface for the coated NPs in SEM (**Figure S8E**) clearly indicates the change in morphology and the 'bumps' on the surface may indicate binding pockets 'binding pockets'. The darker spots in HRTEM (Figure S7A and S7B) and the brighter spots in STEM images (**Figure 2D** in the main article and **Figure S8B**) clearly show the presence of gold nanoparticle on the surface. The AuNP-HSA specially binds onto the 'binding pockets' and thus the small spots may indicate the nanopockets.

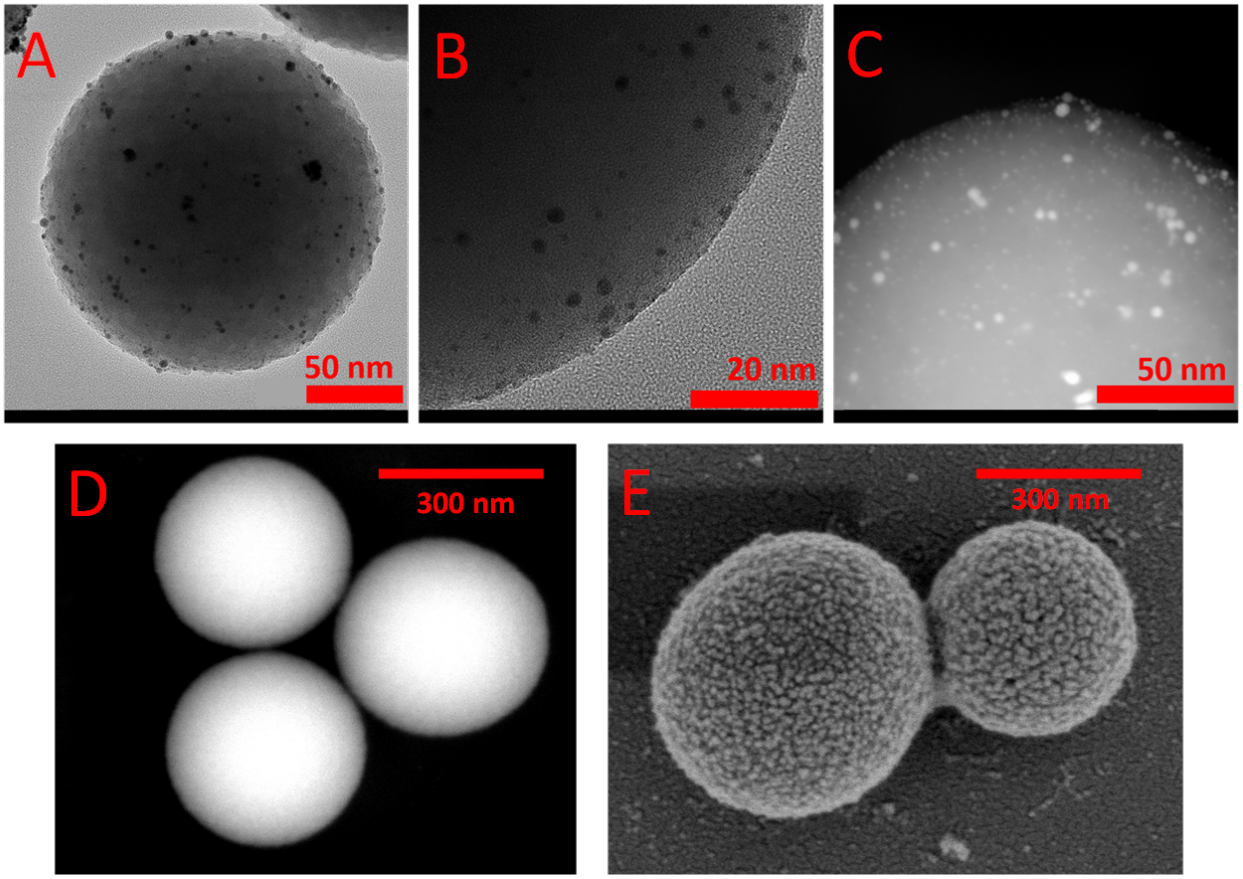

Figure S8. AuNP-HSA conjugate was bound onto the NPs and electron microscopy was performed to locate the binding pockets. The darker spots in Figure A and B represents AuNPs in HRTEM images after AuNP-HSA conjugate bound on NPs. In Figure C, the brighter images represents the same AuNPs. These spots in A to C clearly indicate nanopockets. The smooth surface in Figure D (SEM image) represents the uncoated, bare nanoparticles whereas for coated NPs (E), the surface is rough after the polymerization reaction with features that could possibly include binding sites (SEM image).

Mass Spectrometry analysis. Mass spectrometry was performed on human serum, albumin depleted serum by ProteoExtract and albumin depleted human serum by PEG-coated nano pockets (NP) to qualitatively and quantitatively analyze the albumin depletion ability from human serum. All the samples were analyzed using a Dionex Ultimate 3000 UHPLC interfaced to a QSTAR® Elite mass spectrometer (AB Sciex) in positive ion mode. In brief, samples of human serum before and after depletion were separated using ProSwift™ RP-10R monolithic column via a 15 min gradient and analyzed using TOF (time of flight) mass spectrometry. The HSA was expected to be eluted at ~ 11.4 min as indicated by pure HSA. The extracted ion chromatograms of HSA showed both the ProteoExtract and NP resulted in ~82-90% removal of

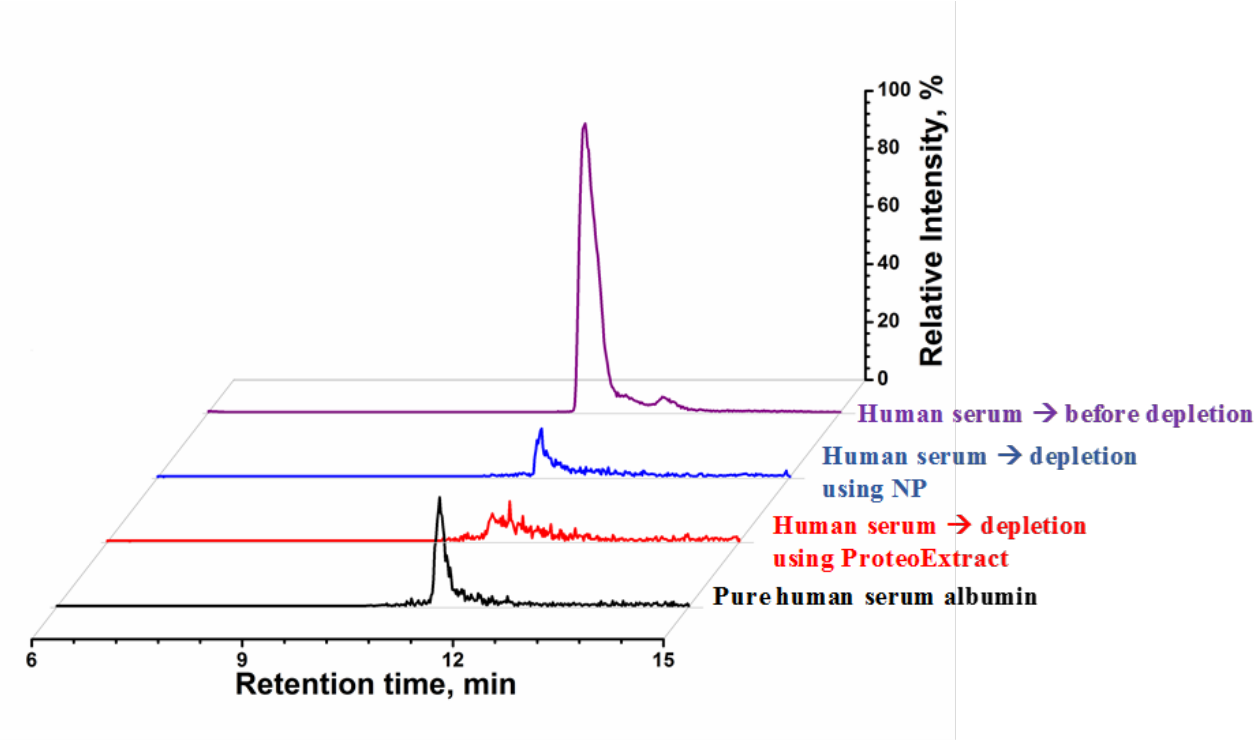

albumin from human serum by calculating the peak area **(Figure S9**).

Figure S9. Extracted ion chromatograms of HSA for human serum, albumin depleted human serum by ProteoExtract and NP, pure human serum using ProSwift™ RP-10R monolithic column and a 15 min gradient. The area of peak ~11.4 min indicated the amount of HSA in the samples.

Specificity studies. We tested selectivity and specificity of our nanopockets (NP) to selectively deplete human serum albumin from human serum samples. To demonstrate that our nanopockets do not non-specifically bind to low abundant proteins, we spiked human serum

with 10 ng mL^{-1} of Prostate specific antigen. We compared the relative abundance of PSA in the spiked serum samples, NP treated serum spiked sample and ProteoExtract (PE) treated spiked serum sample. Electrochemiluminescence (ECL) based immunoassay was used to detect PSA selectively from spiked human serum samples. Briefly, we attached captured antibodies on to single walled carbon nanotube surface on pyrolytic graphite chip. These capture antibodies for PSA selectively capture PSA from our serum samples and ECL label RuBPY silica nanoparticles coated with detection antibodies specific to PSA were allowed to incubate to form a sandwich immunoassay. By applying potential of 1.0 V vs Ag/AgCl in presence of co-reactant tripropylamine ECL was captured using a CCD camera. The relative ECL intensities were obtained for all the three samples. The spiked PSA in human serum vs the sample treated with NP have ECL signal 1.02 X compared to their controls whereas the ProteoExtract treated serum samples 1.25 X times ECL signal suggesting that removal of HSA has slightly enriched the low abundant proteins in the samples but haven't deplete any low abundant proteins non-specifically. Thus, our methodologies can be applied to proteomics and biosensor platforms where there is need for enrichment of low abundant proteins for sensitive detection of protein from the complex serum matrix.

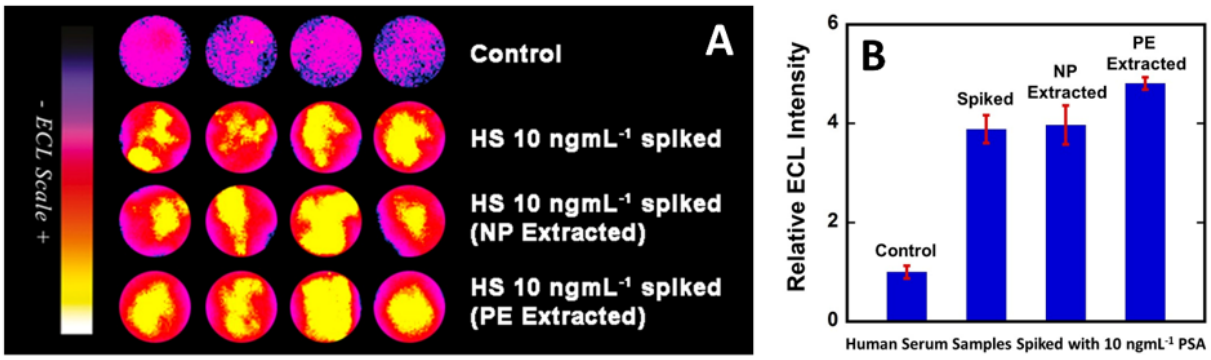

Figure S10. ECL results for spiked human serum samples when treated with nanopockets and proteoextract columns. A) Recolorized ECL images showing ECL responses of four different samples. control with no PSA spiked, 10 ng mL^{-1} spiked human serum sample, 10 ng mL^{-1} spiked human serum sample followed by human serum albumin extracted via nanopockets, 10 ng mL^{-1} spiked human serum sample followed by human serum albumin extracted via proteoextract columns. B) Bar graph showing relative ECL responses when compared to control for 3 different spiked samples before and after NP and PE extraction of human serum albumin.

FT-IR Studies. Fourier transform-infrared spectroscopy (FT-IR) were collected using a Nicolet Magna 560 spectrometer equipped with a TGS detector. A total of 64 scans were collected at the range of 500-4000 cm^{-1}. The presence of carbonyl band confirmed the protein on surface in addition to other protein quantification methods **(Figure S10**).

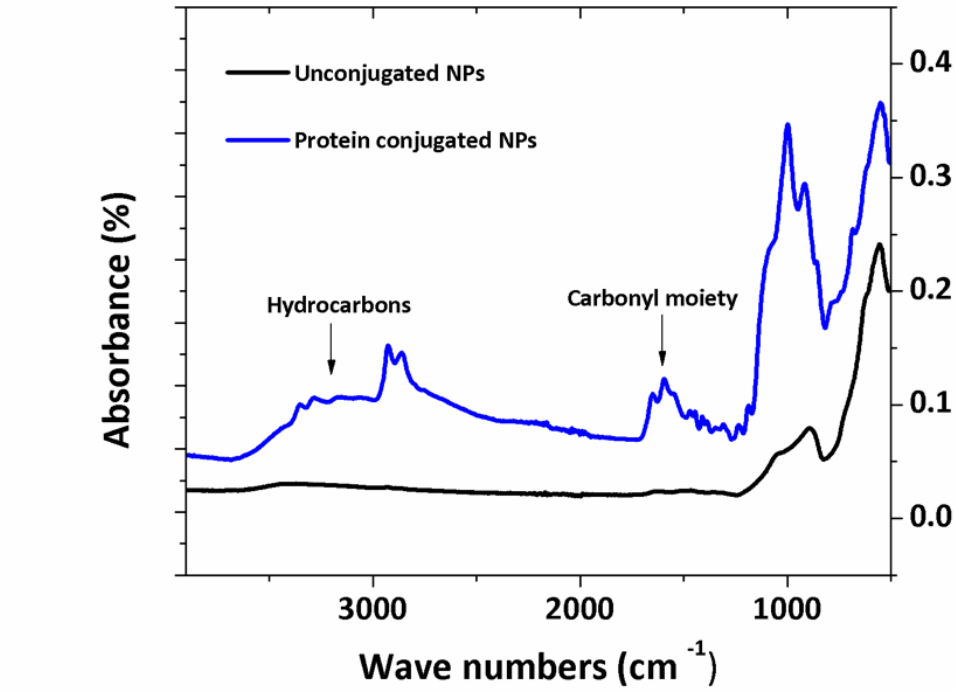

Figure S11. FT-IR spectra for protein-binding NPs and Protein-conjugated NPs. The amind I amnde II bands between 1700 and 1500 cm_{-1} confirms the presence of protein bound to the surface nanopockets of NPs. (For protein amine frequencies, see J. F. Rusling and T. F. Kumosinski, *Nonlinear Computer Modeling of Chemical and Biochemical Data*, Academic Press, San Diego, 1996, Chapter 7)

XPS Analysis of the NPs. The surface of the nanomaterials was further analyzed by X-ray photoelectron spectroscopy (XPS), a Quantum 2000 spectrometer with scanning ESCA microprobe (Physical Electronics Industries Inc.), using Al-K radiation (=1486.6 eV) as the radiation source. The powder samples were pressed on carbon tape mounted on adhesive copper tape stuck to a sample stage placed in the analysis chamber. The obtained XPS spectra were analyzed and fitted using CasaXPS software (version 1 It 2.3.12). The C 1s photoelectron line at 284.6 eV was used as a reference for correction of the surface charging. A mixture of

Gaussian (70 %) and Lorentzian (30 %) functions was used for the least-squares curve fitting procedure. **Figure S12** confirmed the presence of importance elements such as Si, Fe, N, O and C on the surface probably from the amine groups, hydroxyl groups, other hydrophobic groups such as benzyl, propyl, ethyl etc.

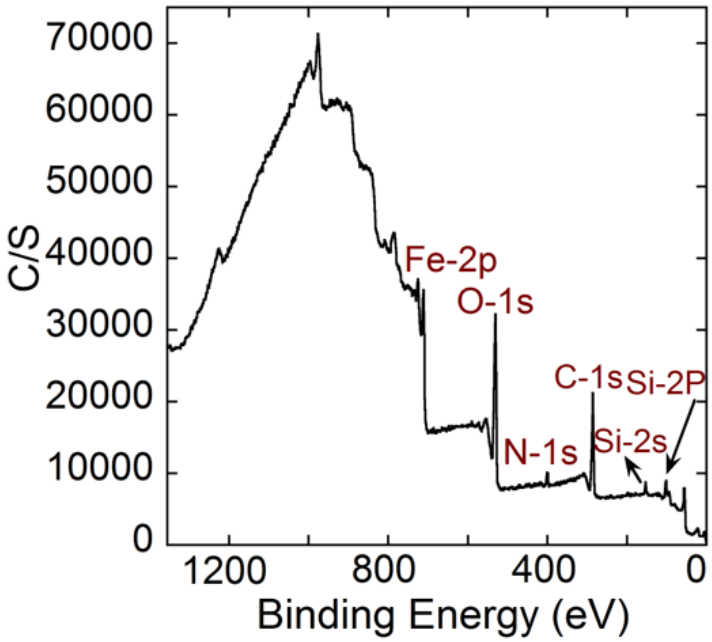

Figure S12. XPS spectra for protein-binding NPs. The presence of N, Si, O, C confirm the presence different functional groups such as amine, hydroxyl, propyl, benzyl groups etc.

Probable mechanism of removal of HSA from HSA-binding NPs. The HSA-binding NPs behave like an antibody and thus bind with HSA in an antigen-antibody binding fashion. There are several types of non-covalent interaction occurs between NPs and HSA. The reason behind choosing different types of silanes is to increase selectivity via. Incorporating amino acid like groups in addition to size and shape interaction. Like in antigen-antibody interaction, there is possibilities of H-bonding interaction, ionic interaction, hydrophobic interaction, van der Waals interaction in this case as well (**Figure S13**).

To remove HSA from the system, we used sodium hydroxide solution or glycine at pH 2.5. In acidic and basic medium, the highly positive charge or negative charge break all the interaction

mentioned above. The glycine solution dissociates most protein-protein interaction without much affecting protein structure, thus it was used in reusability studies.

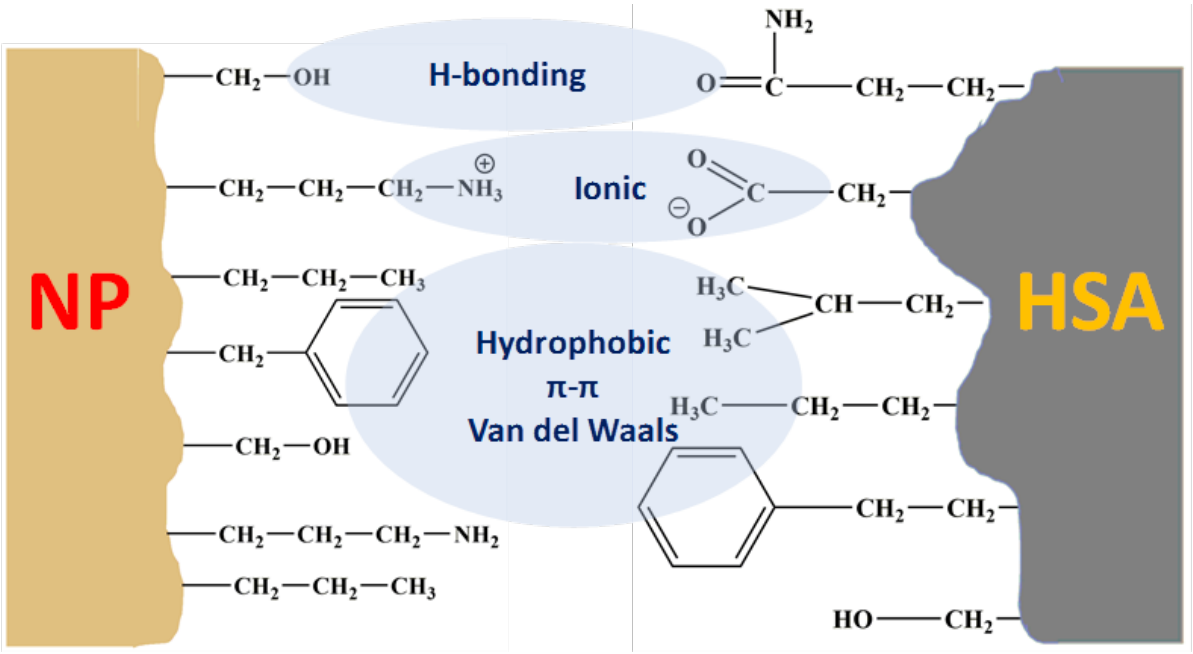

Figure S13. Schematic representation showing different types of possible interactions between HSA-binding NPs and HSA.

Calculation of protein contamination after each use. The amount of HSA or proteins remains on the NPs after each use was measured using BCA assay. In each case, at least 5 times washing was done using phosphate buffer and then BCA solution was added on the particle. The particles were very clean with no 'protein' bound on the surface. **Figure S14a** describes the absorption intensity of BCA solution at 562 nm after each use. The intensity was also measured after protein conjugation after each use. The higher absorption intensity confirmed the presence of protein on the surface (**Figure S14 b**).

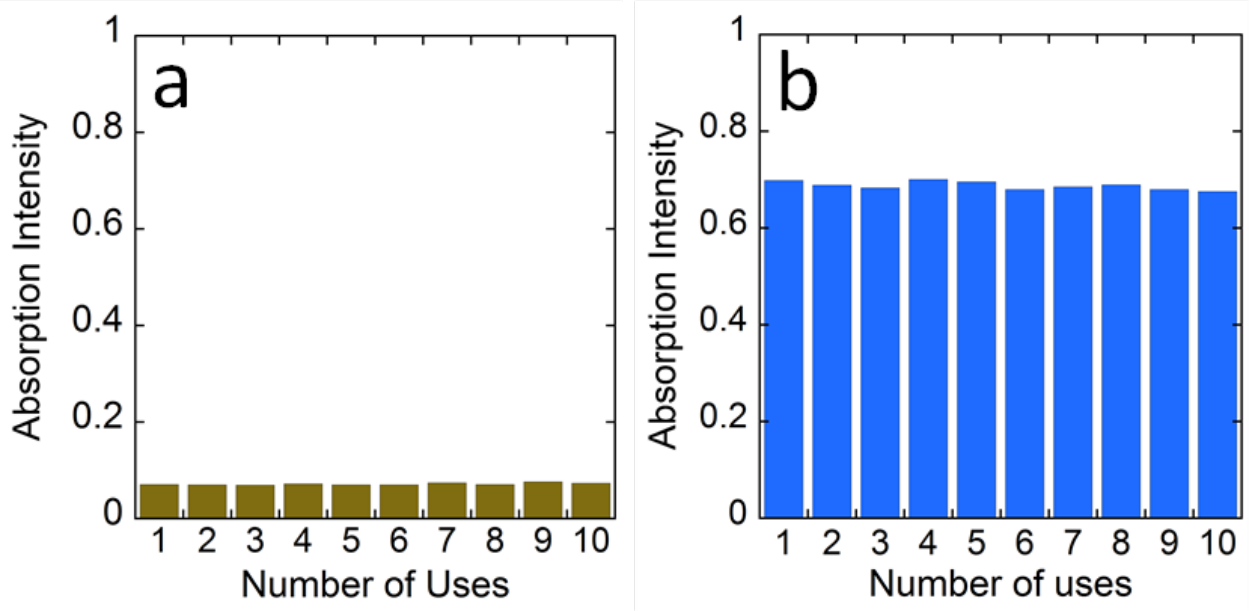

Figure S14. Absorption intensity of the washed NPs after each use. BCA solution was added and intensity was measured at 562 nm to measure amount of protein on the surface. There was no protein on the sample after extensive washing (Figure a) and Figure b confirms the presence of proteins.

Table S4. List of references showing the thicker polymer coating while reatinign good binding

coating	Target protein	Polymers used	Support	Reference
~190 nm (from DLS) no microscopy data	Lysozyme	Metal chelating monomers	Silica NP	Li, W., Sun, Y., Yang, C., Yan, X., Guo, H., Fu, G *ACS Appl. Mater. Interfaces* **2015**, *7*, 27188−27196.
55.8 to 181 nm	Albumin	poly(ethylene-co-vinyl alcohol)	Magnetic NP	Lee, M. H., Ahluwalia, A., Hsu, K. M., Chin, W. T., Lin, H. Y. *RSC Adv.* **2014**, *4*, 36990–36995.
20 nm	Bovine hemoglobin	Dopamine	Magnetic NP	Jia, X., Xu, M., Wang, Y., Ran, D., Yang, S., Zhang, M. *Analyst* **2013**,*138*, 651–658.
15-16 nm	Hemoglobin	Mixture of silanes	Silica NP	Shiomi, T., Matsui, M., Mizukami, F., Sakaguchi, K. *Biomat.* **2005**, *26*, 5564–5571

100 nm	HRP	3-amino- phenylboronic acid (APBA)	polystyrene microtiter plates	Bossi, A., Piletsky, S. A., Piletska, E. V., Righetti, P. G., Turner, A. P. *Anal. Chem.* **2001**, *73*, 5281-5286.
50 nm	BSA	Acrylamide and their derivatives	Silica coated magnetic np	Li, X., Zhang, B., Li, W., Lei, X., Fan, X., Tian, L., Zhang, H., Zhang, Q. *Biosensors and Bioelectronics* **2014**, *51*, 261-267
15-20 nm	Papain	Dopamine	Carbon nanotubes	Liu, R., Sha, M., Jiang, S., Luo, J., Liu, X. *Talanta* **2014**, *120*, 76-83
50-55 nm	HSA	polydopamine	Carbon nanotubes	Yin, Y., Yan, L., Zhang, Z., Wang, J. *Talanta* **2015**, *144* 671-679

References.

1. J. M. Walker, *The protein protocols Handbook*, Springer, 2009.
2. J. Y. Yoon, H. M. Park, J. H. Kim and W. S. Kim, *J. Colloid Interface Sci.* 1996, **177**, 613-620.
3. J. Y. Yoon, J. H. Kim and W. S. Kim, Colloids Surfaces A, 1999, **153**, 413-419.
4. Reichert Technol. Application Note 1: Human Serum Albumin (HSA) Binding to Biotinylated Anti-HSA lgG Captured on Planar Neutravidin Surface. http://www.reichertspr.com/clientuploads/directory/application_notes/1-Reichert SPR Biotinylated Anti-HSA-HSA Binding.pdf
5. B. D. Hames, *Gel electrophoresis of proteins: a practical approach,* OUP, Oxford, 1998.
6. S. Bhakta, M. S. I. Seraji, S. L. Suib and J. F. Rusling, *ACS Appl. Mater. & Inter,* 2015, **7**, 28197-28206.
7. K. Rezwan, A. R. Studart, J. Voros and L. J. J. Gauckler, *Phys. Chem. B*, 2005, **109**, 14469−14474.
8. H. Cai, Y. Wang, Y. Yu, M.V. Mirkin, S. Bhakta, G.W. Bishop, A.A. Joshi and J.F. Rusling, *Anal. Chem.* 2015, **87**, 6403-6410.
9. M. A. Kiseley, I. A. Gryzunov, G. E. Dobretsov, M. N. Komarova, *Biofizika*, 2001, **46**, 423-427.
10. V. Mani, D. P. Wasalathanthri, A. A. Joshi, C. V. Kumar and J. F. Rusling, *Anal. Chem.*, 2012, **84**, 10485−10491.
11. K. Kadimisetty, S. Malla, N. P. Sardesai, A. A. Joshi, R. C. Faria, N. H. Lee and J. F. Rusling, *Anal. Chem.,* 2015, **87**, 4472-4478